Seismic design of non-structural components mounted on irregular reinforced concrete buildings

Ayad B. Aldeka[1], Nikolaos I. Tziavos[2], Michaela Gkantou[3], Samir Dirar[4*] and Andrew H.C. Chan[5]

[1]Senior Lecturer, Nottingham Trent University, Nottingham, NG1 4FQ, UK
[2]Research Associate, University of Cambridge, Cambridge, CB3 0FA, UK
[3]Senior Lecturer, Liverpool John Moores University, Liverpool, L2 2QP, UK
[4]Associate Professor, University of Birmingham, Edgbaston, Birmingham, B15 2TT, UK
[5]Professor, University of Tasmania, Sandy Bay, TAS 7005, Australia

[*]Corresponding author, Email: s.m.o.h.dirar@bham.ac.uk

Abstract

The seismic response of non-structural components (NSCs) attached to irregular reinforced concrete (RC) multi-storey buildings is underestimated by current European design provisions. This paper presents a new design model for NSCs, accounting for the effect of torsion and seismic capacity of an irregular RC primary structure (P-structure). The proposed model is a modification of the current Eurocode 8 (EC8) model for the acceleration amplification factor of NSCs. It is based on the results of some 5000 nonlinear dynamic finite element analyses conducted on thirty-three building cases. The finite element analyses covered a wide range of parameters including plan layout, seismic capacity, fundamental vibration period, total height, floor rotation, ground type and eccentricity ratio. The proposed model has been demonstrated to be an improvement over EC8 model, especially for NSCs mounted on the flexible side and in tune with the fundamental vibration period of a P-structure.

Keywords: design; Eurocode 8; irregular buildings; non-structural components; torsion

1. Introduction

Non-structural components (NSCs) are members or devices attached to a building without substantial contribution to its load resisting system. For instance, architectural elements such as walls, partitions or façades are classified as NSCs along with mechanical and electrical devices, also known as acceleration-sensitive components. In the aftermath of earthquake events, it has been recognised that damage to NSCs could significantly affect occupants' quality of life and have drastic consequences on the operation of residential and industrial structures (McKevitt, 2004). Therefore, accurate prediction of the seismic performance of NSCs using seismic codes such as Eurocode 8 (EC8) (2004), ASCE (2010), and UBC (2012) is of utmost importance in order to ensure both safety and functionality.

Studies on the dynamic behaviour of architectural components attached to primary structures (P-structures) have been reported by Yang and Huang (1993, 1998), Agrawal (1999), Agrawal and Datta (1999a, 1999b), Mohammed *et al*. (2008), Johnson *et al*. (2016), Lim *et al*. (2017), and Sousa and Monteiro (2018). However, our understanding of the behaviour of acceleration-sensitive NSCs attached to irregular reinforced concrete (RC) P-structures is still relatively limited. Lima and Martinelli (2019) examined the mechanical parameters governing the performance of acceleration-sensitive NSCs. Upon performing a nonlinear dynamic study on RC buildings, Petrone *et al*. (2015) found that EC8 (2004) underestimates the seismic demands of light NSCs for a wide range of excitation frequencies. Focussing on irregular RC multi-storey buildings, Aldeka *et al.* (2014a, 2014b, 2015) studied the response of acceleration-sensitive NSCs attached along the heights of irregular P-structures by means of nonlinear dynamic finite element analyses (FEA) and demonstrated that EC8 (2004) underestimates the performance of NSCs. Mohsenian *et al.* (2019) investigated the seismic demand of non-structural components and concluded that currently employed design codes may underestimate the accelerations applied to NSCs by up to 80%. Based on published data, Filiatrault and Sullivan (2014) emphasised the lack of accuracy when designing NSCs under seismic actions. Similarly, Martinelli and Faella (2016) presented an overview of seismic code rules suggesting that current design equations could not predict adequately the interaction between the P-structures and NSCs. Most recently, Anajafi and Medina, (2018, 2019) examined the floor spectra of instrumented buildings in order to evaluate the effects of torsional flexibility on the seismic design of non-structural components. They concluded that significant torsional response can result in increased NSCs seismic demand, particularly for NSCs at a floor

periphery and away from elements of the lateral-force resisting systems. Moreover, they showed that parameters like floor diaphragm flexibility, vertical irregularity in mass and stiffness, and seismic base isolation can affect NSCs accelaration demand. Surana et al. (2018) studied the torsional effects of hill-side RC buildings with irregular configurations and proposed spectral amplification functions that can take into account the effect of the buildings' plan and elevation irregularities on the response of NSCs. In the absence of codified provisions for hill-side buildings, they suggested that the proposed functions could be used for seismic design of acceleration-sensitive NSCs for a given structure, ground motion response spectrum and NSC location.

Aiming to address the gap in current seismic design codes, this paper presents a new design expression that improves the predictions of the current EC8 (2004) model for the design of acceleration-sensitive NSCs. It takes into consideration the maximum seismic capacity and the torsional behaviour of P-structures. The new design model is calibrated and validated against the results of some 5000 nonlinear dynamic FEA of NSCs attached to irregular RC buildings. The design data are presented in Section 3. A proposal for modifying EC8 (2004) design model for NSCs is presented in Section 4. The proposed model is assessed in Section 5 on the basis of FEA results for an extensive range of P-structures.

2. Research significance

In seismic codification, acceleration amplification factors are used in the design of NSCs to guarantee safe and functional designs. This approach ensures that NSCs of critical importance, such as medical, electrical and mechanical equipment, are designed in such a way that they remain fully functional under seismic actions in lifeline structures such as hospitals, power plants, and factories. However, the design of acceleration-sensitive NSCs is currently underestimated by design codes. Damage of such NSCs could pose risk to human life and result in significant economic losses. Hence it is deemed essential that NSCs be designed to withstand earthquake action without damage. This paper proposes a new model for the design of acceleration-sensitive NSCs that takes into account the effect of the torsional response and the maximum seismic capacity of P-structures.

3. Design data

This section gives an overview of the numerical results which formed the basis for the development, calibration and validation of a new seismic design model for NSCs. For this purpose, a comprehensive data-set comprising 5194 nonlinear dynamic FEA was utilised. The numerical models cover a series of geometries and parameters, which are presented in Section 3.1. The key results along with the main modelling considerations are briefly described in Section 3.2. Further details on the development of the FE models and numerical implementation can be found in Aldeka *et al.* (2014a, 2014b, 2015).

3.1. Geometries and parameters

The main aim of the numerical investigations was to quantify the response of NSCs under seismic actions. Therefore, a wide range of buildings with varying heights, ground types and eccentricity ratios were considered from the authors' previous studies (Aldeka et al., 2014a; 2014b; 2015), resulting in a total of thirty-three irregular RC P-structures. The NSCs considered were elastic, lightweight, acceleration-sensitive components, such as mechanical equipment found in industrial buildings, electrical components found in commercial buildings or medical equipment found in healthcare centres. The investigated P-structures were categorised into four groups of buildings.

Group 1 (G1) comprised four irregular three-storey RC P-structures with a common plan layout and a total height of 9 m. G1-1 was designed to resist vertical loads only, whereas G1-2 and G1-3 were designed according to EC8 (2004). Type 1 spectrum for ground type C and a design ground acceleration (a_g) of 0.15 g and 0.25 g, respectively was employed. The values of the over-strength factor (γ_{Rd}) for G1-2 and G1-3 did not satisfy the global and local ductility requirements recommended by EC8 (2004), hence, G1-4 which conforms to EC8 (2004) Ductility Class M requirements was also included in the group. The concrete class was C25/30 and the steel reinforcement was Grade 400 for all G1 buildings except for G1-1 which had steel reinforcement with a nominal yield strength of 459 MPa (Rozman and Fajfar 2009).

Group 2 (G2) comprised five irregular RC P-structures with the same plan layout and storey height (i.e., 3 m) as G1 buildings. In this case the total height was modified, resulting in 5-, 7, 10-, 13- and 15- storey buildings designated as G2-1, G2-2, G2-3, G2-4 and G2-5. The group was designed according to EC8 (2004) Ductility Class M requirements using Type 1 spectrum

for ground type C, a_g value of 0.25 g and a behaviour factor (q) of 3.45. Concrete Class C25/30 and steel reinforcement Class C S500 were used.

In Group 3 (G3), the ground type (A, B, D, E) was varied as per EC8 (2004) for four different heights. Four irregular RC P-structures (G3-1, G3-2, G3-3 and G3-4) with the same plan layout as G1-1 and four different heights ranging from 9 to 45 m were examined resulting in a total of 16 RC P-structures. An elastic response spectrum consistent with Type 1 was applied. The behaviour factor was taken equal to 3.45 and the design acceleration for Type A ground was taken equal to 0.25 g.

Finally, in Group 4 (G4), the effect of eccentricity ratio (R) on the response of eight three-storey RC buildings was assessed. The investigated P-structures (G4-1 to G4-8) had R values of 0.0, 0.026, 0.060, 0.098, 0.143, 0.205, 0.284, and 0.372, respectively, in two perpendicular horizontal directions (i.e. $R_x = R_y$). As shown in Fig. 1(b), the P-structures had a single bay of 5.5 m in both X and Y directions and square column cross-sections. The design of G4 P-structures was carried out according to Eurocodes EC1 (2002), EC2 (2004), and EC8 (2004).

The plan layouts of the modelled buildings are shown in Fig. 1, where the eccentricities between their centres of rigidity (CR) and centres of mass (CM) are also shown. In this paper, the eccentricity ratio in a given direction is defined as the static eccentricity in that direction divided by the elasticity radius. Initially, the CM coordinates (g_x, g_y) were calculated as follows:

$$g_x = \frac{\sum_N^{i=1}(w_i \,.\, x)}{\sum_N^{i=1} w_i} \tag{1}$$

$$g_y = \frac{\sum_N^{i=1}(w_i \,.\, y)}{\sum_N^{i=1} w_i} \tag{2}$$

where N is the number of the structural members, w_i is the weight of a structural member, and x and y are the member coordinates. Subsequently, the CR coordinates (l_x, l_y) were calculated as follows using the lateral stiffness of the structural members, K_x and K_y:

$$\ell_x = \frac{\sum(K_y . x)}{\sum K_y} \tag{3}$$

$$\ell_y = \frac{\sum(K_x . y)}{\sum K_x} \tag{4}$$

K_x and K_y were calculated using MIDAS Gen ver. 2.1 (2012). The reader is referred to

MIDAS Gen (2012) Analysis Manual for further details. The static eccentricity in a given direction was calculated as follows:

$$e_x = |\ell_x - g_x| \tag{5}$$

$$e_y = |\ell_y - g_y| \tag{6}$$

The torsional stiffness, K_R of a structure about its centre of rigidity, CR is given by:

$$K_R = \sum (K_x . \bar{Y}^2) + (K_y . \bar{X}^2) \tag{7}$$

where $\bar{X}$ and $\bar{Y}$ may be calculated as:

$$\bar{X} = x - \ell_x \tag{8}$$

$$\bar{Y} = y - \ell_y \tag{9}$$

The radii of elasticity in the two horizontal directions (r_{ex} and r_{ey}) were calculated as follows:

$$r_{ex} = \sqrt{\frac{K_R}{\sum K_x}} \tag{10}$$

$$r_{ey} = \sqrt{\frac{K_R}{\sum K_y}} \tag{11}$$

Finally, the eccentricity ratios R_{ex} and R_{ey} in X and Y directions, respectively, were calculated as follow:

$$R_{ex} = e_y / r_{ex} \tag{12}$$

$$R_{ey} = e_x / r_{ey} \tag{13}$$

It should be noted that the eccentricity ratios reported in this paper correspond mainly to the top floors of the P-structures. For the analysis and interpretation of the numerical results, the following key characteristic design parameters were evaluated for each group: a) the fundamental vibration periods of the P-structures and the NSCs, b) the maximum seismic capacities of the P-structures and c) the top-floor rotations. A summary of the characteristic design parameters for each model is given in Table 1.

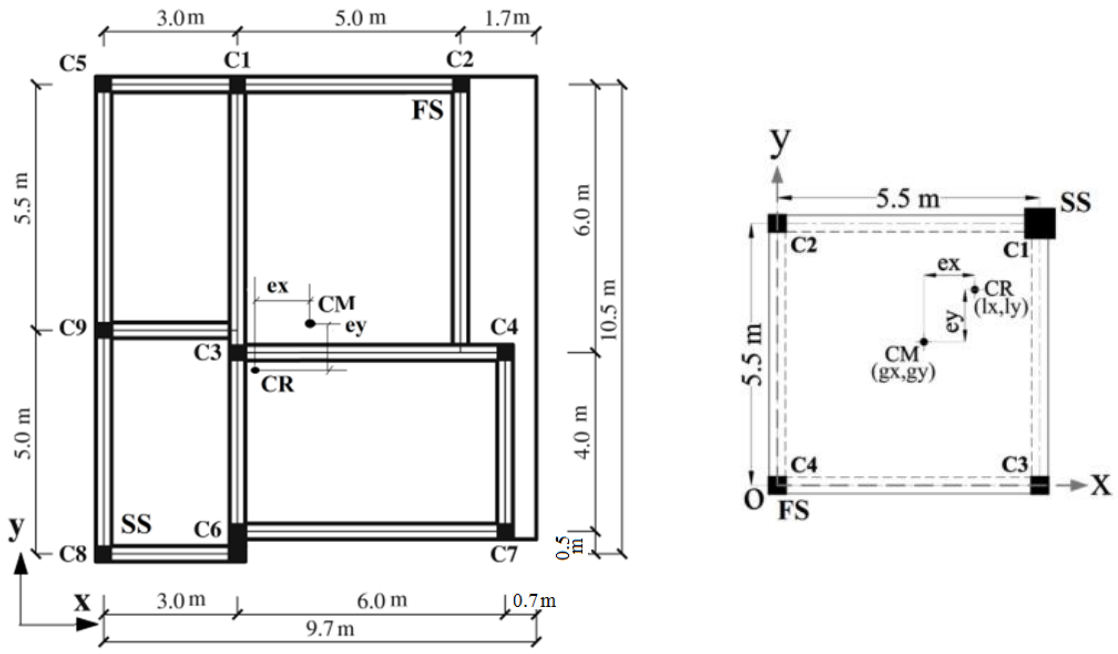

a) Groups 1, 2, 3 (G1, G2, G3) b) Group 4 (G4)

Fig. 1: Plan layouts of modelled P-structures (Aldeka *et al*., 2014a, 2014b, 2015)

3.2. Modelling considerations and key results

For the thirty-three cases (Aldeka *et al*., 2014a, 2014b, 2015) presented in Section 3.1, the finite element program MIDAS Gen ver. 2.1 (2012) was employed to conduct nonlinear dynamic analyses. The P-structures were modelled using distributed inelastic fibre elements. The concrete behaviour was defined using the confined and unconfined concrete models proposed by Mander *et al*. (1988) whereas the steel reinforcement was modelled using the analytical model by Menegotto and Pinto (1973) for cyclic loads. Natural and artificial earthquake records comprising 70 accelerograms were adopted for the selected analyses. REXEL software (Iervolino *et al*., 2010) from the European Strong-motion Database (ESD) was used to obtain the natural records. SIMQKE code (Gelfi, 2007) was used to generate artificial records. A NSC was modelled as a fixed vertical cantilever with a lumped mass at its free end. This approach has been widely adopted in previous studies (see e.g., Sackman and Kelly, 1979; Yang and Huang, 1998; Agrawal, 1999; Mohammed *et al*. 2008; Chauduri and Villaverde, 2008; Opropeza *et al*., 2010). The vibration period (T_C) of the NSC matched one of the first three vibration periods (T_1, T_2, or T_3) of the P-structure. Based on the recommendation by Graves and Morante (2006), a damping ratio of 3% was employed for the NSCs but further research is recommended to investigate the effect of NSC damping ratio on

175 the accuracy of design model predictions. For further details on the validation of the nonlinear
176 dynamic FE model, the reader is referred to Aldeka *et al*. (2014a). In total, 5194 nonlinear
177 dynamic FEA were carried out and form the basis of the calibration and validation of the new
178 design model presented in this paper.

179 In Table 1, key results are listed along with the labelling used in the references, the updated
180 notation applied in this paper, and the ground type for each case. In particular, Tc, the
181 fundamental vibration period of the NSCs; and T_1, T_2, and T_3; the first three vibration periods
182 of the P-structures, are reported. T_1 and T_2 refer to the translational mode periods whereas T_3
183 refers to the torsional mode period. For Groups 1 and 4, NSCs with fundamental vibration
184 periods similar to the first three vibration periods of the P-structures were considered. In Group
185 2, T_1 and T_2 were approximately equal hence NSCs with fundamental vibration periods similar
186 to T_1 and T_3 were considered. In Group 3, NSCs with $Tc = T_1$ were considered.

187 The elastic and maximum (F_{SC}) seismic capacities of the P-structures in [g] are also given
188 in Table 1. The elastic and maximum seismic capacities were calculated using the extended N2
189 procedure. This is a simplified nonlinear method for the seismic analysis of plan-asymmetric
190 structures. In the extended N2 procedure, the results of a three-dimensional nonlinear static
191 (push-over) analysis are combined with the results of a modal analysis of a two-dimensional
192 model. The extended N2 method has been demonstrated to provide reasonable predictions of
193 the torsional influences in asymmetric structures (Fajfar, 2002; Fajfar et al., 2005a; Kreslind
194 and Fajfar, 2013; Stefano and Pintucchi, 2010).

195

196 Table 1: Key results from collated data.

	Labelling of Reference	Notation herein	Ground type	Fund. period, T [s]	Elastic Capacity factor [g]	Max. Capacity factor [g] F_{SC}	Top rotation, θ [rad]	$F_{T\ mean}$ Eq. (14)	T_C		
									T_1	T_2	T_3
Group 1 (Aldeka *et al*., 2014a)	Test	G1-1	--	0.82	0.070	0.26	0.0084	1.36	0.82	0.73	0.65
	Test 0.15	G1-2	C	0.82	0.100	0.46	0.0084	1.36	0.82	0.73	0.65
	Test 0.25	G1-3	C	0.82	0.120	0.51	0.0077	1.33	0.82	0.73	0.65
	EC8 M	G1-4	C	0.55	0.135	0.76	0.0038	1.16	0.55	0.52	0.42
Group 2 (Aldeka *et al*., 2014a)	EC8 M5	G2-1	C	0.66	0.160	0.74	0.0045	1.19	0.66	-	0.51
	EC8 M7	G2-2	C	0.84	0.160	0.69	0.0059	1.26	0.84	-	0.66
	EC8 M10	G2-3	C	1.17	0.160	0.63	0.0090	1.39	1.17	-	0.92
	EC8 M13	G2-4	C	1.29	0.170	0.58	0.0106	1.46	1.29	-	1.02
	EC8 M15	G2-5	C	1.39	0.170	0.58	0.0117	1.51	1.39	-	1.12
Group 3 (Aldeka *et al*., 2014b)	EC8 M3	G3-1A	A	0.620	0.120	0.69	0.0052	1.23	0.62	-	-
		G3-1B	B	0.590	0.131	0.72	0.0046	1.20	0.59	-	-
		G3-1D	D	0.470	0.149	0.83	0.0024	1.10	0.47	-	-
		G3-1E	E	0.520	0.143	0.79	0.0029	1.13	0.52	-	-
	EC8 M5	G3-2A	A	0.750	0.142	0.64	0.0067	1.29	0.75	-	-
		G3-2B	B	0.710	0.156	0.68	0.0057	1.25	0.71	-	-
		G3-2D	D	0.610	0.179	0.78	0.0032	1.14	0.61	-	-
		G3-2E	E	0.660	0.160	0.74	0.0047	1.20	0.66	-	-
	EC8 M10	G3-3A	A	1.250	0.135	0.57	0.0102	1.44	1.25	-	-
		G3-3B	B	1.220	0.150	0.59	0.0096	1.42	1.22	-	-
		G3-3D	D	1.080	0.178	0.70	0.0057	1.25	1.08	-	-
		G3-3E	E	1.170	0.160	0.63	0.0091	1.39	1.17	-	-
	EC8 M15	G3-4A	A	1.500	0.148	0.50	0.0163	1.71	1.50	-	-
		G3-4B	B	1.450	0.168	0.54	0.0140	1.61	1.45	-	-
		G3-4D	D	1.280	0.192	0.64	0.0081	1.35	1.28	-	-
		G3-4E	E	1.390	0.170	0.58	0.0117	1.51	1.39	-	-
Group 4 (Aldeka *et al*., 2015)	Reference (R_x=R_y=*0.000*)	G4-1	C	0.385	0.15	0.57	0.0000	1.00	0.385	0.379	0.261
	Modified 1 (R_x=R_y=*0.026*)	G4-2	C	0.385	0.14	0.57	0.0003	1.01	0.385	0.379	0.261
	Modified 2 (R_x=R_y=*0.060*)	G4-3	C	0.385	0.14	0.56	0.0007	1.03	0.385	0.379	0.261
	Modified 3 (R_x=R_y=*0.098*)	G4-4	C	0.385	0.14	0.55	0.0013	1.06	0.385	0.379	0.261
	Modified 4 (R_x=R_y=*0.143*)	G4-5	C	0.385	0.14	0.55	0.0022	1.10	0.385	0.379	0.261
	Modified 5 (R_x=R_y=*0.205*)	G4-6	C	0.385	0.15	0.55	0.0038	1.16	0.385	0.379	0.261
	Modified 6 (R_x=R_y=*0.284*)	G4-7	C	0.385	0.15	0.54	0.0072	1.31	0.385	0.379	0.261
	Modified 7 (R_x=R_y=*0.372*)	G4-8	C	0.385	0.15	0.54	0.0114	1.49	0.385	0.379	0.261

197

198

4. Proposed model for the seismic design of NSCs

Aldeka *et al.* (2014a, 2014b, 2015) demonstrated that, at the design PGA of the P-structures, EC8 (2004) underestimates the acceleration response of NSCs with T_C equal to T_1 and attached to the flexible sides of the top floors by about 35%. Similarly, an underestimation of about 52% was observed at the PGA values corresponding to the maximum seismic capacities of the P-structures. This is attributed to the fact that EC8 (2004) does not explicitly account for the increase in NSCs accelerations caused by the torsional behaviour of the P-structures.

In Eq. (14) the relationship between the torsional amplification factor for NSCs accelerations (F_T) and the rotation (θ) of the top floor is given, as presented by Aldeka *et al.* (2014a), for NSCs with T_C equal to T_1. The torsional amplification factor (F_T) is defined as the ratio of the peak component acceleration at the flexible side ($PCA_{xy,FS}$) to the corresponding value at the centre of the rigidity ($PCA_{xy,CR}$). PCA_{xy} is computed as the square root of the sum of the squares of PCA_x and PCA_y. PCA_x and PCA_y are the peak component acceleration (PCA) values in the horizontal x and y directions, respectively. Eq. (14) was used to quantify F_T for the thirty-three cases reported in Section 3.1 and the results are presented in Table 1.

$$F_T = 43.3\theta + 1.0 \quad (14)$$

Eq. (14) calculates F_T as a function of θ only. However, in the proposed design model (see Eq. (17)), a linear variation of F_T along the height of a P-structure is considered by multiplying F_T with z/H (i.e., the relative position of NSCs).

Even though the behaviour of NSCs can be influenced by the P-structure torsional response, this is currently not considered by EC8 (2004) provisions. In particular, Section 4.3.5.2 of EC8 (2004) suggests Eq. (15) for calculating the NSC acceleration amplification factor:

$$\frac{S_a}{\alpha S} = \left[\frac{3[1+(z/H)]}{1+[1-(T_c/T_1)]^2} - 0.5\right] \quad (15)$$

where

S_a: seismic coefficient applicable to NSC

α: the ratio of the design ground acceleration on type A ground to the acceleration of gravity

S: soil factor (S is taken as 1.0, 1.2, 1.15, 1.35, or 1.40 for ground types A, B, C, D, or E, respectively, considering Type 1 elastic response spectrum of EC8)

T_C: fundamental vibration period of the NSC

T_1: fundamental vibration period of the P-structure (in the examined direction)

z: height of the NSC above the level of application of the seismic action and

H: building height measured from the level of application of the seismic action.

Utilising the FE results of the NSCs attached to Group 1 buildings, the underconservative nature of Eq. (15) is demonstrated in Fig. 2, which shows the variations of the acceleration amplification factor (A_p^a) with T_C/T_1. The acceleration amplification factor (A_p^a) is defined as PCAxy/PGA for the NSCs attached to the flexible sides of the top floors. Fig. 2 also compares the results of the NSCs attached to Group 1 buildings (G1-1, G1-2, G1-3 and G1-4) with the predictions of Eq. (15). Although G1-1, G1-2 and G1-3 had the same fundamental periods (see Table 1), their NSCs acceleration response increased with the maximum seismic capacities of P-structures (F_{SC}). Eq. (15) conservatively predicted the response of the NSCs attached to G1-1, which was designed for gravity loads only. Moreover, as also shown in Fig. 2 and explained in Aldeka *et al*. (2014a, 2014b, 2015), the response of NSCs with $T_C \approx 0$s (i.e., rigid NSCs) could be adequately predicted by Eq. (15). However, as can also be observed in Fig. 2, Eq. (15) significantly underestimated the amplification factors for NSCs with T_C/T_1 values in the range of 0.68 to 1.0. Similar trends to those presented in Fig. 2 were reported by Aldeka *et al*. (2014a, 2014b, 2015). Hence evaluating the NSCs behaviour using only the fundamental vibration period can lead to inaccurate estimations. This is more pronounced in Zone 2 than in Zones 1 and 3 (see Fig. 2), where Zones 1, 2 and 3 correspond to $0 \leq T_C/T_1 \leq 0.68$, $0.68 \leq T_C/T_1 \leq 1.0$, and $1.0 \leq T_C/T_1 \leq 2.5$, respectively. Hence, Eq. (15) is hereinafter modified in such a way that it better predicts the acceleration response of NSCs attached to irregular RC P-structures.

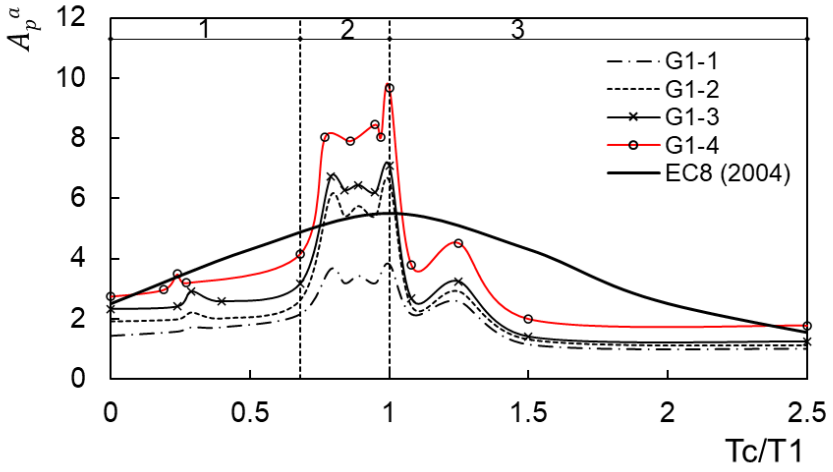

Fig. 2: Acceleration amplification factor (A_p^a) for varying NSC to P-structure period ratio (T_C/T_1)

In order to take into consideration the torsional amplification factor (F_T) along with the maximum seismic capacity (F_{SC}) of the P-structure, Eq. (15) is modified based on statistical calibration of the FE results of Group 1 buildings. The parameters F_T and F'_{SC} are incorporated into Eq. (16) in such a way that its predictions are in agreement with the FE results of the NSCs in Zone 2 (see Fig. 2).

$$\frac{S_a}{\alpha S} = \left[\frac{6[1 + (z/H)]F_T F'_{SC}}{1 + [1 - (T_c/T_1)]^2} - 0.5\right] \tag{16}$$

The dimensionless parameter F'_{SC} is the maximum seismic capacity (F_{SC}), as defined in Table 1, divided by the acceleration of gravity [g]. In order to avoid overestimating the acceleration response of rigid NSCs (i.e., with T_C = 0s), which are adequately predicted by Eq. (15) as can be seen in Fig. 2, Eq. (16) is further modified by multiplying the term $(1 - (T_C/T_1)^2)$ with the term $(4F_T F'_{SC} - 1)$. This ensures an acceleration amplification value of 2.5 for rigid NSCs (i.e., similar to that predicted by Eq. (15) as can be seen in Fig. 3). Eq. (16) is futher calibrated on the basis of the FE results of the NSCs that are out-of-tune with the first three vibration periods of the P-structures by applying an exponent of 3/5 to the term $(1 - (T_C/T_1)^2)$. Hence, Eq. (16) can be re-written as follows:

$$\frac{S_a}{\alpha S} = \left[\frac{6[1 + (z/H)]F_T F'_{SC}}{1 + (4F_T F'_{SC} - 1)([1 - (T_c/T_1)]^2)^{3/5}} - 0.5\right] \tag{17}$$

Figs. 3(a) to 3(d) present the variations of the acceleration amplification factor (A_p^a) with T_C/T_1 for Group 1 buildings. The FE results are compared with the predictions of EC8 (2004) (i.e., Eq. (15)) and Eq. (17). It is shown that Eq. (17) provides improved estimations for the NSCs attached to the top floors of G1 buildings. In addition, as shown in Fig. 3(a), Eq. (17) correctly predicts lower acceleration response than EC8 (2004) for the case of the NSCs attached to building G1-1. This better prediction is made possible by Eq. (17) taking into consideration the relatively low maximum seismic capacity of building G1-1 (0.26 g). Overall, Eq. (17) provides better estimations compared with EC8 (2004) (i.e., Eq. (15)) for the NSCs attached to Group 1 buildings, demonstrating adequate calibration.

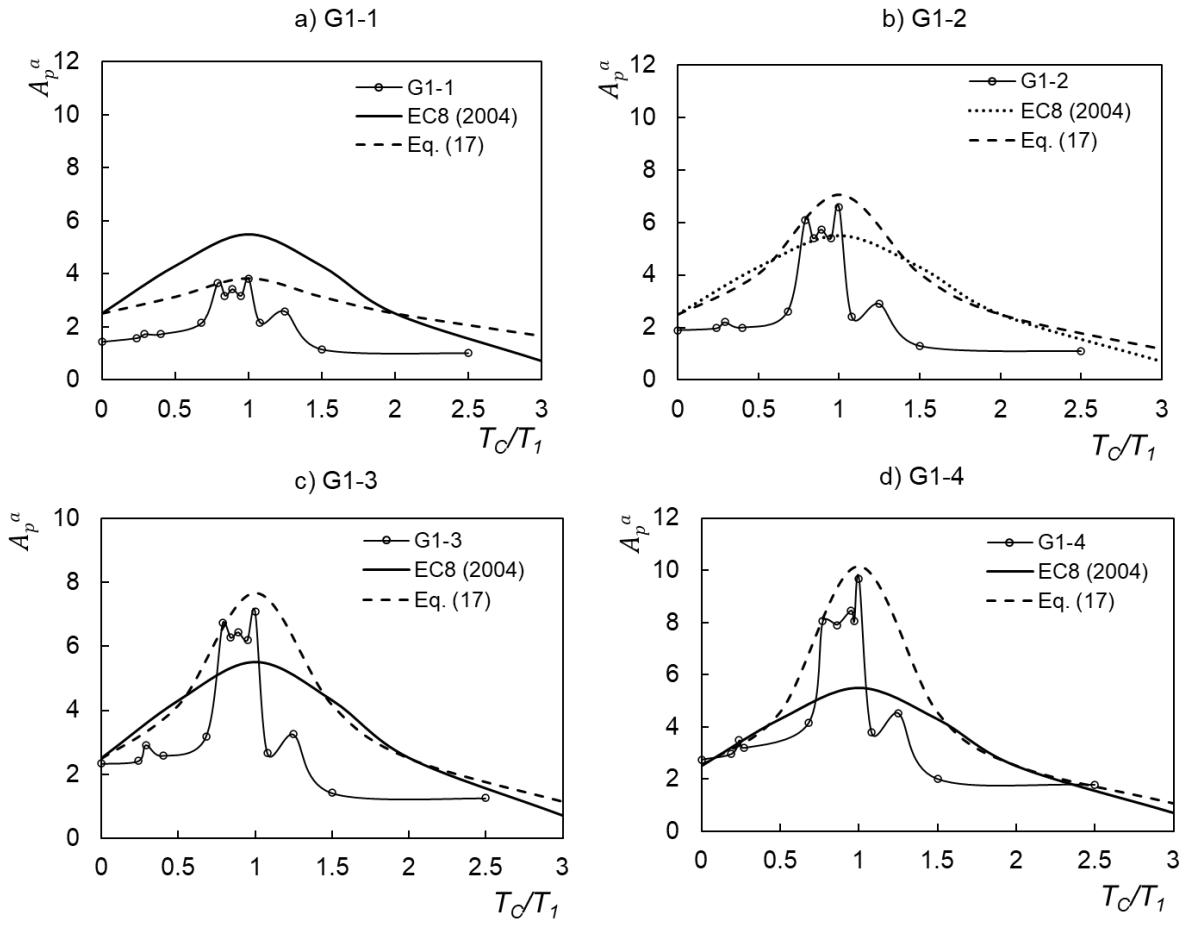

Fig. 3: Acceleration amplification factor (A_p^a) versus NSC to P-structure period ratio (T_C/T_1)

5. Assessment of the proposed design model

In this section, the assessment of the proposed design model (i.e., Eq. (17)) is presented. The proposed design model differs from current EC8 (2004) design provisions (i.e., Eq. (15)) in that Eq. (17) takes into consideration the torsional behaviour and the maximum seismic capacity of the P-structure. Thus, in order to use Eq. (17), the values of F_T and F_{SC} are required. For a given P-structure, a pushover analysis gives F_{SC} together with the rotation (θ) of the top floor. Once θ is known, Eq. (14) may be used to calculate F_T.

In the following sections, the accuracy of the proposed design model is assessed using the FE results of the NSCs attached to the buildings in Groups 2, 3 and 4. The FE results of Group 1 buidlings were not used in the assessment because they were used to calibrate the design model.

5.1. Effect of P-structure height

In Group 2, the focus was on the effect of P-structure height on the response of NSCs attached to irregular RC buildings. The suitability of the proposed design model (i.e., Eq. (17)) for predicting the seismic response of the NSCs attached to G2 buildings is assessed in this section. Figs. 4-6 compare the predictions of Eq. (17) with the FE-predicted acceleration amplification factors (A_p^a) for the NSCs at the centre of rigidity (CR) and on the flexible side (FS). The results are presented as a function of z/H, where z and H are as defined in Section 4.

For rigid NSCs, Fig. 4 shows that the proposed model yields safe predictions for A_p^a values at the centre of rigidity. The model predictions are mostly accurate for A_p^a values on the flexible side. For buildings G2-3, G2-4 and G2-5, with 10, 13 and 15 stories, respectively, A_p^a values at the lower third of the buildings are slightly underestimated (by a maximum value of 17%) compared with the FE results. In order to prevent any damage in these cases, it is suggested that the design of NSCs is performed using A_p^a values at z/H = 1.0. As illustrated in Fig. 5, the predictions of the proposed model provides an upper bound on A_p^a values for the NSCs with T_C equal to T_1. For the NSCs with periods equal to the torsional fundamental period of the P-structure (i.e., T_C=T_3), as depicted in Fig. 6, the predictions for the flexible sides are mainly accurate, especially at upper floors, whereas for the NSCs at the centre of rigidity, a conservative outcome is observed.

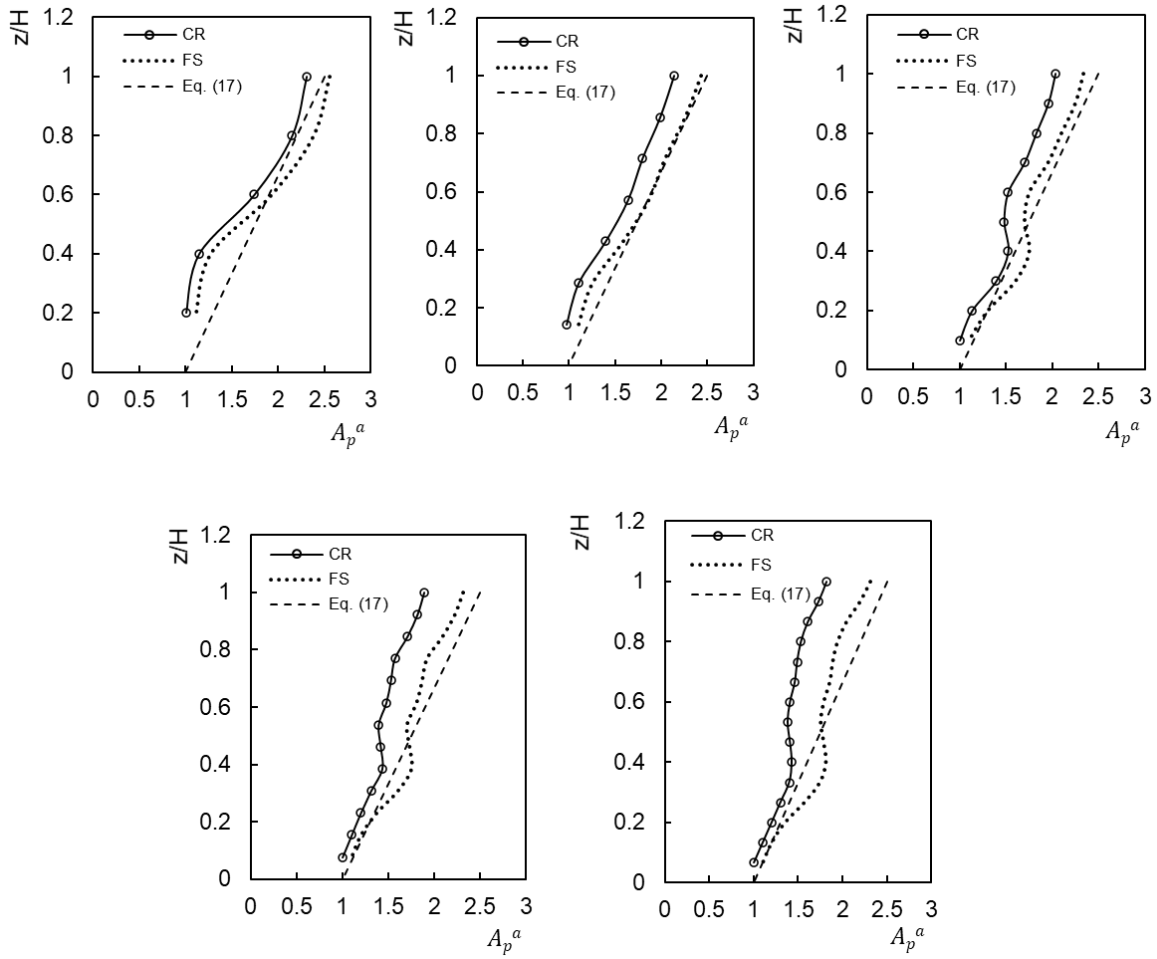

Fig. 4: Comparison between FE-predicted acceleration amplification factors (A_p^a) and predictions of Eq. (17) for rigid NSCs ($T_C \approx 0$ s)

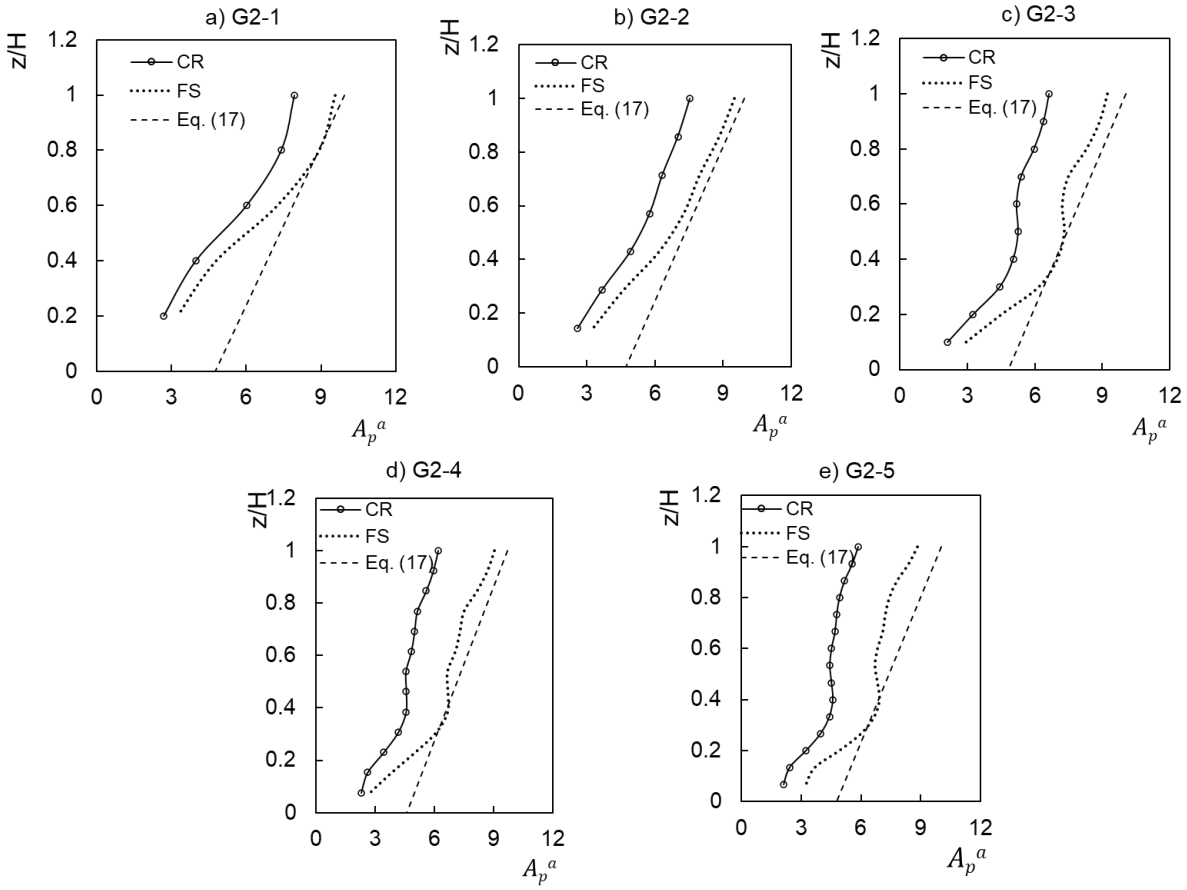

311

312 Fig. 5: Comparison between FE-predicted acceleration amplification factors (A_p^a) and

313 predictions of Eq. (17) for NSCs with T_C=T_1

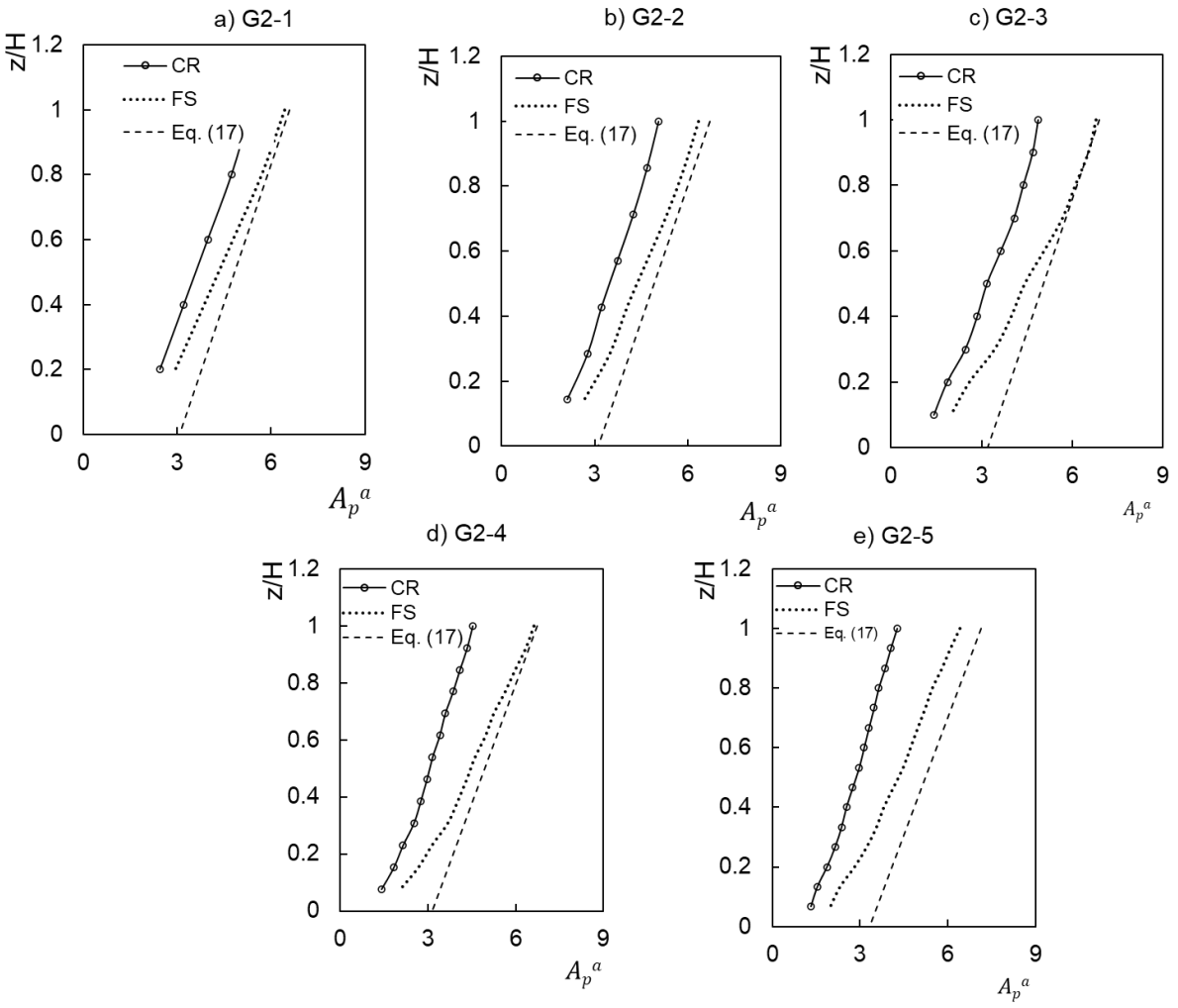

Fig. 6: Comparison between FE-predicted acceleration amplification factors (A_p^a) and predictions of Eq. (17) for NSCs with T_C=T_3

Table 2 shows the comparison between EC8 (2004) and Eq. (17) predictions for the NSCs with $T_C = T_1$ and attached to the flexible side of the top floors of G2 buildings. To demonstrate the improved safety offered by the proposed model over that offered by EC8 (2004) model, the predictions of the two design models are compared with the NSCs acceleration results at PGA values corresponding to the maximum sesismic capacities of G2 buildings. Table 2 shows that, for the considered NSCs, EC8 (2004) underestimates the peak acceleration response by 50% on average. On the contrary, Eq. (17) offers improved performance and the predictions of the NSCs peak accelerations are improved by 41% on average (i.e., an average analytical-to-FE ratio of 91%). Overall, Figs. 4-6 and Table 2 demonstrate clearly the suitability of Eq. (17) for predicting the seismic response of NSCs attached to irregular RC P-structures with different heights.

Table 2: Comparison between EC8 (2004) and Eq. (17) predictions for NSCs with $T_C = T_1$ and attached to the top floors of irregular RC buildings with different heights.

Building	PCA_{xy} (FEA) [g]	S_a (EC8) [g]	S_a (Eq. (17)) [g]	$\frac{S_a(EC8)}{PCA_{xy}(FEA)}$	$\frac{S_a(Eq.(17))}{PCA_{xy}(FEA)}$
G2-1	3.17	1.58	2.89	0.50	0.91
G2-2	3.05	1.58	2.86	0.52	0.94
G2-3	3.20	1.58	2.88	0.49	0.90
G2-4	3.10	1.58	2.78	0.51	0.90
G2-5	3.15	1.58	2.88	0.50	0.91
Average				0.50	0.91
Standard deviation				0.01	0.02

5.2. Effect of ground type

The effect of various ground types was also considered for the assessment of the proposed design model. This is based on the FE results of Group 3 where the effect of ground types A, B, D and E on the seismic response of NSCs attached to the flexible side of the top floors of G3 buildings was studied.

Table 3 shows the comparison between EC8 (2004) and Eq. (17) predictions for the NSCs with $T_C = T_1$ at PGA values corresponding to the maximum sesismic capacities of G3 buildings. As can be seen in Table 3, Eq. (17) is much safer than EC8 (2004) model. Eq. (17) underestimates the peak acceleration response of the NSCs attached to the buildings on ground types A, B, and D by about 16%, 10%, and 13% on average, respectively. For ground type E, Eq. (17) overestimates the peak acceleration response by approximately 9% on average. On the contrary, EC8 (2004) model underestimates the peak response of the NSCs for the four investigated ground types by 39 to 45%. Overall, Eq. (17) has a mean predicted-to-FE ratio of 0.93 and a standard deviation of 0.10 whereas EC8 (2004) has a corresponding values of 0.52 and 0.05, respectively.

Table 3: Comparison between EC8 (2004) and Eq. (17) predictions for NSCs with $T_C = T_1$ and attached to the top floors of irregular RC buildings on different ground types.

Building	PCA_{xy} (FEA) [g]	S_a (EC8) [g]	S_a (Eq. (17)) [g]	$\frac{S_a(EC8)}{PCA_{xy}(FEA)}$	$\frac{S_a(Eq.(17))}{PCA_{xy}(FEA)}$
G3-1A	2.92	1.38	2.42	0.47	0.83
G3-1B	3.37	1.65	2.96	0.49	0.88
G3-1D	4.11	1.86	3.53	0.45	0.86
G3-1E	3.34	1.93	3.57	0.58	1.07
G3-2A	2.85	1.38	2.35	0.48	0.82
G3-2B	3.25	1.65	2.91	0.51	0.90
G3-2D	3.99	1.86	3.43	0.47	0.86
G3-2E	3.22	1.93	3.55	0.60	1.10
G3-3A	2.82	1.38	2.34	0.49	0.83
G3-3B	3.21	1.65	2.87	0.51	0.89
G3-3D	3.95	1.86	3.38	0.47	0.86
G3-3E	3.24	1.93	3.50	0.60	1.08
G3-4A	2.73	1.38	2.44	0.51	0.89
G3-4B	3.18	1.65	2.98	0.52	0.94
G3-4D	3.80	1.86	3.33	0.49	0.88
G3-4E	3.15	1.93	3.50	0.61	1.11
Average				0.52	0.93
Standard deviation				0.05	0.10

5.3. Effect of eccentricity ratio of the P-structure

Further to previous sections, the accuracy of the proposed model is herein assessed against the FE results of NSCs attached to RC buildings with different eccentricity ratios. Fig. 7 presents the variation of A_p^a values on the flexible side (FS) of G4 buildings at PGA values corresponding to the elastic seismic capacities of the P-structures. Fig. 7 also compares the predictions of the proposed model and EC8 (2004) with the FE results. For G4-1 with $R_x = R_y = 0$ (i.e., regular building), both design models give safe predictions at $T_C = T_1$, with the proposed model overestimating the A_p^a value at $T_C = T_1$ by 14.9%. However, with increasing the eccentricity ratio from 0.026 (G4-2) to 0.372 (G4-8), EC8 (2004) model increasingly underestimates A_p^a values at $T_C = T_1$ from 9.4% (G4-2) to 36.9% (G4-8). Conversely, the proposed model gives consistently accurate predictions at $T_C = T_1$ for all irregular buildings, with a mean predicted-to-numerical ratio of 1.04 and a standard deviation of 0.03. As explained earlier in this paper, EC8 (2004) model does not take into consideration the effect of P-structure torsional behaviour and therefore underestimates the acceleration response of the NSCs attached to irregular buildings. On the other hand, the accurate predictions of Eq. (17) confirm that the proposed model adequately considers the effect of P-structure torsional behaviour.

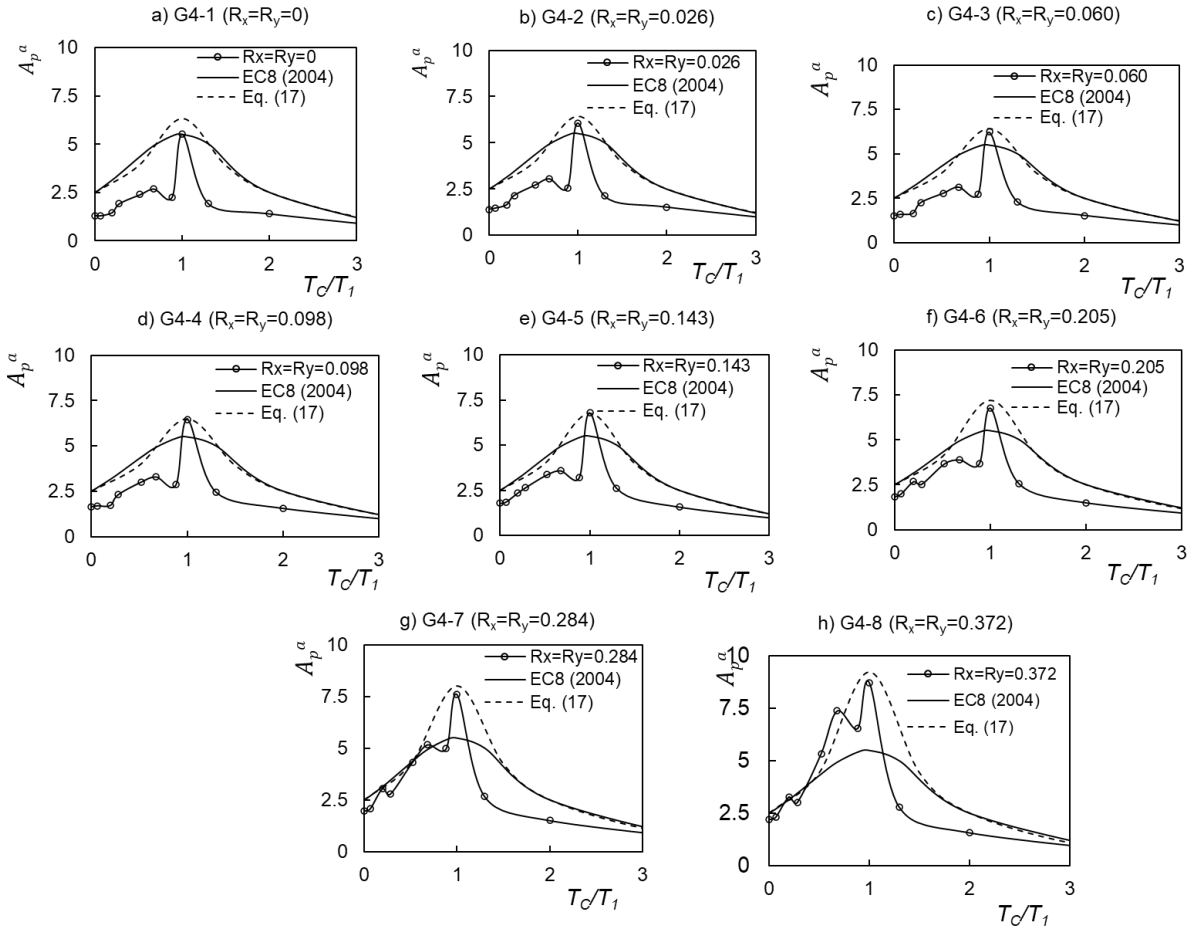

Fig. 7: Comparison between acceleration amplification factors (A_p^a) and the predictions of Eq. (17) for NSCs attached to G4 buildings

6. Conclusions

This paper presents a new Eurocode-based model for the design of NSCs attached to irregular RC P-structures. The propsed model accounts for both the torsional behaviour and the maximum seismic capacity of an irregular RC P-structure. The new model is based on the results of more than 5000 nonlinear dynamic FEA of NSCs attached to irregular RC P-structures with different plan layouts, seismic capacities, total heights, ground types and eccentricity ratios. A subset of the FE results was used to calibrate the proposed model and another subset was used for model validation purposes.

Comparison between the FE results and EC8 (2004) predictions showed that, under tuned conditions, EC8 (2004) design model underestimates the acceleration response of NSCs on the flexible side of irregular RC P-structures. The gap between the FE results and EC8 (2004) predictions increased from 9.4 to 36.9% with increasing the eccentricity ratio from 0.026 to

0.372. On the other hand, the proposed design model has been demonstrated to be an improvement over EC8 (2004) design provisions, particularly for NSCs on the flexible side and in tune with the fundamental vibration period of the P-structure.

A parametric study was carried out to assess the effect of P-structure height, ground type, and eccentricity ratio of the P-structure on the accuracy of the predictions of the proposed model. For the vast majority of cases, the proposed model provided safe estimates for the acceleration response of NSCs attached to different heights. For NSCs in tune with the fundamental vibration periods of the P-structures, the proposed model accurately predicted the variation of NSCs acceleration response with ground type or P-structure eccentricity ratio with mean predicted ratios of 0.93 and 1.04, and standard deviations of 0.10 and 0.03, respectively.

Declaration of competing interest

The authors declare that they have no known competing financial interests or personal relationships that could have appeared to influence the work reported in this paper.

Acknowledgments

The FE results presented in this paper were obtained using the University of Birmingham High Performance Computing facility (BlueBEAR).

References

Agrawal, A.K. (1999), "Non-linear response of light equipment system in a torsional building to bi directional ground excitation", *Shock Vib.*, **6**(5), 223-236.

Agrawal, A.K. and Datta, T. (1999a), "Seismic behavior of a secondary system on a yielding torsionally coupled primary system", *J. Seismol. Earthq. Eng.*, **2**(1), 35-46.

Agrawal, A.K. and Datta, T. (1999b), "Seismic response of a secondary system attached to a torsionally coupled primary system under bi-directional ground motion", *J. Earthq. Technol. - ISET*, **36**(1), 27-42.

Aldeka, A.B., Chan, A.H.C. and Dirar, S. (2014a), "Response of non-structural components mounted on irregular RC buildings: comparison between FE and EC8 predictions", *Earthq. Struct.*, **6**(4), 351-373.

Aldeka, A.B., Dirar, S., Chan, A.H.C. and Martinez-Vazquez, P. (2015), "Seismic response of non-structural components attached to reinforced concrete structures with different

410 eccentricity ratios", *Earthq. Struct.,* **8**(5): 21pp.
411 Aldeka, A.B., Dirar, S., Martinez-Vazquez, P. and Chan, A.H.C. (2014b), "Influence of ground
412 type on the seismic response of non-structural components integrated on asymmetrical
413 reinforced concrete buildings", In: *Proceedings of the Australian Earthquake Engineering*
414 *Society 2014 Conference*, Nov 21 -23, Lorne, Victoria, 11pp.
415 Anajafi, H. and Medina, R.A., 2018, June. Effects of Supporting Building Characteristics on
416 Nonstructural components Acceleration Demands. In 11th US National Conference on
417 Earthquake Engineering.
418 Anajafi, H. and Medina, R.A. (2019) Lessons learned from evaluating the responses of
419 instrumented buildings in the United States: The effects of supporting building
420 characteristics on floor response spectra. Earthquake Spectra, 35(1), pp.159-191.
421 ASCE (2010), *Minimum design loads for buildings and other structures*, American Society of
422 Civil Engineers*,* ASCE/SEI Standard 7-10, Reston, VA.
423 Chaudhuri, S.R. and Villaverde, R. (2008), "Effect of building nonlinearity on seismic response
424 of nonstructural components: a parametric study", *J. Struct. Eng.,* ASCE*,* **134**(4), 661-670.
425 EC1 (2002), EN 1991-1-1 Eurocode 1, *Actions on structures, Part 1-1: General actions –*
426 *Densities, self-weight, imposed loads for buildings*, European Committee for Standardization,
427 Brussels, Belgium.
428 EC2 (2004), EN 1992-1-1 Eurocode 2, *Design of concrete structures, Part 1-1: General rules*
429 *and rules for buildings*, European Committee for Standardization, Brussels, Belgium.
430 EC8 (2004+A1:2013), EN 1998-1 Eurocode 8, *Design of structures for earthquake resistance,*
431 *Part 1: General rules, seismic actions and rules for buildings*, European Committee for
432 Standardization, Brussels, Belgium.
433 Fajfar, P. (2002). Structural analysis in earthquake engineering - a breakthrough of simplified
434 non-linear methods. In Proceedings of the12th European Conference on Earthquake
435 Engineering, September 9-13, London, UK, 20pp.
436 Fajfar, P., Kilar, V., Marusic, D., Perus, I. and Magliulo, G. (2005a). The extension of the N2
437 method to asymmetric buildings. In Proceedings of the 4th European Workshop on the
438 Seismic Behaviour of Irregular and Complex Structures, August 26-27, Thessaloniki, Greece,
439 16pp.
440 Fajfar, P., Marušić, D. and Peruš, I. (2005b). Torsional effects in the pushover-based seismic
441 analysis of buildings. Journal of Earthquake Engineering, 9 (6): 831-854
442 Filiatrault, A. and Sullivan, T. (2014) "Performance-based seismic design of nonstructural

443 building components: The next frontier of earthquake engineering". *Earthquake Engineering*
444 *and Engineering Vibration*, **13**(1), pp.17-46.
445 Gelfi, P. (2007), "SIMQKE_GR, Programma per la generazione di accelerogrammi artificiali
446 spettro-compatibili", Italy: University of Brescia.
447 Graves, H. and Morante, R. (2006), *Recommendations for revision of seismic damping values*
448 *in Regulatory Guide 1.61*, U.S. Nuclear Regulatory Commission, Office of Nuclear
449 Regulatory Research, Washington.
450 Iervolino, I., Galasso, C. and Cosenza, E. (2010), "REXEL: computer aided record selection
451 for code-based seismic structural analysis", *Bull. Earthq. Eng.*, **8**(2), 339-362.
452 Johnson, T.P., Dowell, R.K. and Silva, J.F. (2016) "A review of code seismic demands for
453 anchorage of nonstructural components" *Journal of Building Engineering*, **5**, pp.249-253.
454 Kreslin, M. and Fajfar, P. (2010). Seismic evaluation of an existing complex RC building.
455 Bulletin of Earthquake Engineering, 8 (2): 363-385
456 Lim, Ellys, Lizhong Jiang, and Nawawi Chouw. "Dynamic response of a non-structural
457 component with three supports in multi-directional earthquakes." *Engineering Structures*
458 **150** (2017): 143-152.
459 Lima, C. and Martinelli, E. (2019) "Seismic Response of Acceleration-Sensitive Non-
460 Structural Components in Buildings". *Buildings*, **9**(1), p.7.
461 Mander, J., Priestley, M.N. and Park, R. (1988), "Theoretical stress-strain model for confined
462 concrete", *J. Struct. Eng.*, ASCE, **114**(8), 1804-1826.
463 Martinelli, E. and Faella, C. (2016) "An overview of the current code provisions on the seismic
464 response of acceleration-sensitive non-structural components in buildings" In *Applied*
465 *Mechanics and Materials*. **847**, 273-280. Trans Tech Publications Ltd.
466 McKevitt, W. (2004), "Reply to the discussion by RD Watts on Proposed Canadian code
467 provisions for seismic design of elements of structures, nonstructural components, and
468 equipment", *Canadian J of Civil Eng.,* **31**(2), 392-392.
469 Menegotto, M. and Pinto, P.E. (1973), "Method of analysis for cyclically loaded RC plane
470 frames including changes in geometry and non-elastic behaviour of elements under
471 combined normal force and bending", *Symposium on the Resistance and Ultimate*
472 *Deformability of Structures acted on by well defined loads*, International Association for
473 Bridge and Structural Engineering, Zurich, Switzerland.
474 MIDAS Gen (2012), *Analysis manual*, version 2.1, http://www.MidasUser.com/.
475 Mohammed, H.H., Ghobarah, A. and Aziz, T.S. (2008), "Seismic response of secondary

systems supported by torsionally yielding structures", *J. Earthq. Eng.*, **12**(6), 932-952.

Mohsenian, V., Gharaei-Moghaddam, N. and Hajirasouliha, I. (2019) "Multilevel seismic demand prediction for acceleration-sensitive non-structural components" *Engineering Structures*, **200**, p.109713.

Negro, P., Mola E., Molina F.J. and Magonette G.E. (2004), "Full-scale PSD testing of a torsionally unbalanced three-storey non-seismic RC frame", In: *Proceedings of 13th World conference on Earthquake Engineering*, Vancouver, Canada, No. 968.

Oropeza, M., Favez, P. and Lestuzzi, P. (2010), "Seismic response of nonstructural components in case of nonlinear structures based on floor response spectra method", *Bull. Earthq. Eng.*, **8**(2), 387-400.

Petrone, C., Magliulo, G. and Manfredi, G. (2015) "Seismic demand on light acceleration-sensitive nonstructural components in European reinforced concrete buildings" *Earthquake engineering & Structural dynamics*, **44**(8), pp.1203-1217.

Rozman, M. and Fajfar, P. (2009), "Seismic response of a RC frame building designed according to old and modern practices", *Bull Earthq. Eng.,* **7**(3): 779-799.

Sackman, J.L. and Kelly, J.M. (1979), "Seismic analysis of internal equipment and components in structures", *Eng. Struct.*, **1**(4), 179-190.

Sousa, L. and Monteiro, R. (2018) "Seismic retrofit options for non-structural building partition walls: Impact on loss estimation and cost-benefit analysis" *Engineering structures*, **161**, pp.8-27.

Stefano, D. M. and Pintucchi, B. (2010). Predicting torsion-induced lateral displacements for pushover analysis: Influence of torsional system characteristics. Earthquake Engineering & Structural Dynamics, 39 (12): 1369-1394.

Surana M, Singh Y, Lang DH. (2018) Effect of irregular structural configuration on floor acceleration demand in hill-side buildings. Earthquake Engng Struct Dyn.;1–23

UBC (2012), *International Conference of Building Officials*, Uniform Building Code. Whittier, California, USA.

Yang, Y.B. and Huang, W.H. (1993), "Seismic response of light equipment in torsional buildings", *Earthq. Eng. Struct. Dyn.*, **22**(2), 113-128.

Yang, Y.B. and Huang, W.H. (1998), "Equipment–structure interaction considering the effect of torsion and base isolation", *Earthq. Eng. Struct. Dyn.*, **27**(2), 155-171